Localized Orbitals in Ethyl Ion and the Perturbation of Ethylene by a Proton. Reaction of Localized Orbitals

David A. Dixon and William N. Lipscomb*

Contribution from the Department of Chemistry, Harvard University, Cambridge, Massachusetts 02138. Received November 16, 1972

Abstract: As a proton approaches along the perpendicular bisector of the C–C line and normal to the plane of ethylene, appreciable orbital perturbations begin at 3.7 Å. Results at the self-consistent field level have been found for a minimum basis set of Slater orbitals using previously obtained equilibrium geometries for both the bridge (C_{2v}) and open ($CH_2CH_3^+$, C_s) structures. Localized orbitals have been obtained by maximizing the self-repulsion energy $\Sigma_i(ii|ii)$ and have been related to the formation of $C_2H_5^+$ from C_2H_4 and a proton, and to the subsequent addition of a nucleophile in the Markovnikov reaction.

The importance of the ethyl cation in the first step of Markovnikov addition reactions, its relative inaccessibility to structure study, and its small size have led to a host of recent theoretical studies.[1–8] Even though much of the attention has centered on whether an open structure (IA) or a bridged structure (IB) is correct, the lack of correlation corrections leaves the answer open at present. An ion cyclotron resonance study is said[9] to favor IA, but if IB were appreciably more stable it could not be eliminated. Effects of substituents on the molecular conformation, including the orientation of CH_2 relative to CH_3 in IA, and the importance of hyperconjugation have also received recent attention.[10,11]

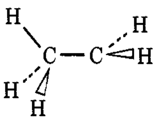
IA

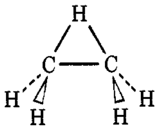
IB

In this paper we derive localized orbitals from the optimized geometries of structures IA and IB using the optimum geometries found by Latham, Hehre, and Pople.[1] We examine the unoccupied (virtual) orbitals useful in the second step of the Markovnikov addition. A study is presented of the variation of the distance of the proton from the center of the CC bond of an undistorted ethylene molecule, from which localized orbitals are also examined. It is found that the proton–ethylene system undergoes a fairly sudden transition, as the proton gradually approaches, from an ethylene molecule perturbed by a proton to an ethyl ion. Various energy results, populations, and other quantities are analyzed for both the optimized geometries (IA and IB) and the proton–ethylene approach. In a later study we hope to extend the basis and to introduce the effects of electron correlation beyond the self-consistent field (SCF) level of the present paper.

Computation

These SCF calculations, carried out with the use of the program written by Stevens,[12] yield the wave function, eigenvalues, and energy. Further analysis of the data was made using the program of Switkes, Hall, and Laws, and the integrals were indexed over molecular orbitals using Marynick's program. The program by Switkes[13] was employed for the conversion of the molecular orbitals to localized orbitals, according to Edmiston and Ruedenberg's procedure[14] which maximizes the self-repulsion energy $\Sigma_i(ii|ii)$. All of these programs were written in this laboratory. All computations were made on the IBM 360–165. For the localizations, a convergence criterion[13] of 0.003 was used.

The geometry of the ground state of ethylene[15] was taken for the part of the study in which the proton approached along R (Chart I) from 13 to 3 au (Table I). This approach was taken along a line perpendicular to the plane of the ethylene and bisecting the C–C distance. For the optimized geometries[1] the coordinates and distances are those shown in Table I and Chart I, respectively.

A minimum basis set of Slater-type orbitals was used having exponents shown in Table I. Except for the added proton, these exponents were taken from those optimized previously[15] in ethylene. In the two optimized geometries the hydrogen exponent was taken as 1.227, while the less strongly bound proton of the R variation (from 13 to 3 au) was taken as 1.1, somewhat closer to the value of 1.0 for a hydrogen atom.

---

(1) W. A. Lathan, W. J. Hehre, and J. A. Pople, *J. Amer. Chem. Soc.*, **93**, 808 (1971).

(2) J. E. Williams, Jr., V. Buss, L. C. Allen, P. v. R. Schleyer, W. A. Lathan, W. J. Hehre, and J. A. Pople, *J. Amer. Chem. Soc.*, **92**, 2141 (1970).

(3) G. V. Pfeiffer and J. G. Jewett, *J. Amer. Chem. Soc.*, **92**, 2143 (1970).

(4) R. Sustman, J. E. Williams, M. J. S. Dewar, L. C. Allen, and P. v. R. Schleyer, *J. Amer. Chem. Soc.*, **91**, 5350 (1969).

(5) F. Fratev, R. Janoschek, and H. Preuss, *Int. J. Quantum Chem.*, **3**, 873 (1969).

(6) T. Yonezawa, H. Nakatasuji, and H. Kato, *J. Amer. Chem. Soc.*, **90**, 1239 (1968).

(7) R. Hoffmann, *J. Chem. Phys.*, **40**, 2480 (1964).

(8) P. C. Hariharan, W. A. Lathan, and J. A. Pople, *Chem. Phys. Lett.*, **14**, 385 (1972).

(9) H. H. Jaffe and S. Billets, *J. Amer. Chem. Soc.*, **94**, 674 (1972).

(10) L. Radom, J. A. Pople, and P. v. R. Schleyer, *J. Amer. Chem. Soc.*, **94**, 5935 (1972).

(11) R. Hoffmann, L. Radom, J. A. Pople, P. v. R. Schleyer, W. J. Hehre, and L. Salem, *J. Amer. Chem. Soc.*, **94**, 6221 (1972).

(12) R. M. Stevens, *J. Chem. Phys.*, **52**, 1397 (1970).

(13) (a) E. Switkes, R. M. Stevens, W. N. Lipscomb, and M. D. Newton, *J. Chem. Phys.*, **51**, 2085 (1969); (b) E. Switkes, W. N. Lipscomb, and M. D. Newton, *J. Amer. Chem. Soc.*, **92**, 3847 (1970); (c) M. D. Newton, E. Switkes, and W. N. Lipscomb, *J. Chem. Phys.*, **53**, 2645 (1970); (d) M. D. Newton and E. Switkes, *ibid.*, **54**, 3179 (1971).

(14) C. Edmiston and K. Ruedenberg, *Rev. Mod. Phys.*, **35**, 457 (1963).

(15) E. Switkes, R. M. Stevens, and W. N. Lipscomb, *J. Chem. Phys.*, **51**, 5229 (1969).

Table I. Coordinates[a] and Exponents

	Coordinates										
	C_2H_4				Optimized, bridge (C_{2v})				Optimized, open (C_s)		
	x	y	z		x	y	z		x	y	z
C(1)	0.0	−1.27558	0.0	C(1)	0.0	−1.32565	0.0	C(1)	0.0	1.40219	0.0
H(1)	1.75113	−2.28659	0.0	H(1)	1.78019	−2.39428	−0.04666	H(1)	1.79369	2.50460	0.05594
				H(5)	0.0	0.0	2.17526	H(3)	1.72516	−2.17785	−0.82024
								H(5)	0.0	−1.84546	2.02503

Proton distances (z direction of planar C_2H_4 geometry)
3, 4, 6, 8, 10, 12, and 13 au

Exponents

H 1s	1.227	
C 1s	5.679	
C 2s	1.751	
C 2p	1.670	
H^+ 1s	1.10 (nonoptimized geometries)	1.227 (optimized geometries, *i.e.*, open and bridge)

[a] The origin is taken at the center of the C–C bond, and coordinates are in atomic units (1 au of distance is 0.5295 Å).

Chart I. Geometries of Molecular Species[c]

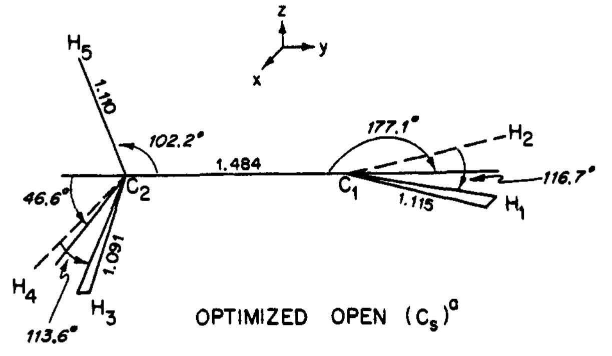

OPTIMIZED OPEN (C_s)[a]

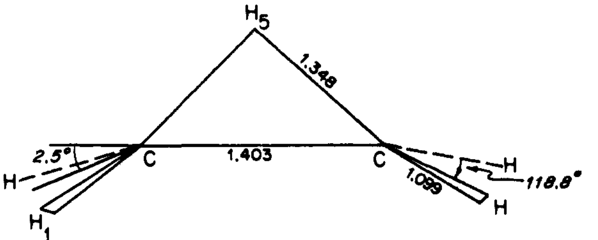

OPTIMIZED BRIDGE (C_{2v})[a]

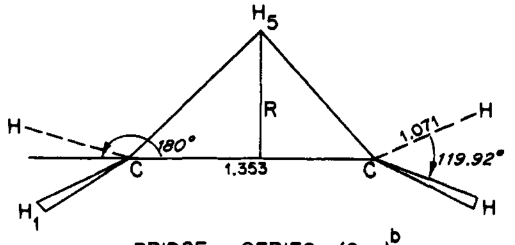

BRIDGE SERIES (C_{2v})[b]

[a] Reference 1. [b] G. Herzberg, "Infrared and Raman Spectra," Van Nostrand, New York, N. Y., 1945, p 439. [c] Atom numbers are referred to in the text.

Energetics

The various SCF energies and virial ratios are given in Table II for both optimized structures (bridge and open), for ethylene, and for the *R* variation. As *R* increases, *i.e.*, as the proton recedes from ethylene, the energy increases in a negative exponential fashion. Both the virial ratio and the comparison of CC in ethylene with that in the optimized bridge structure indicate that the proton must be very close before a noticeable change occurs in the CC bond distance.

We are unable to decide whether the bridged or open structure is the more stable. The optimized geometry yields, with a minimum Slater set having all equal hydrogen exponents and equal exponents on each carbon, an open structure 12 kcal/mol more stable than the bridged structure for $C_2H_5^+$. However, extension of the optimized minimum basis set in the comparison of $2BH_3$ and B_2H_6 favored the double bridge structure of B_2H_6 by 10 kcal/mol,[16,17] and comparison[17] of the probable Hartree–Fock limit (19 kcal/mol) with the experimental dissociation energy of B_2H_6 (35 kcal/mol) indicates that correlation energy favors the bridged structure relative to $2BH_3$ by 8 kcal/mol per hydrogen bridge. Hence, the combination of basis set extension and correlation corrections might lead to stability of the bridged structure relative to the open structure for $C_2H_5^+$. Further studies are in progress.[18]

Recent new optimized geometries[8] of the open and bridged structures for $C_2H_5^+$ are less stable than those previously published[1] in our minimum basis set calculations. However, the energy *difference* between open and bridged structures changes only by 10^{-4} au when these two sets of geometries are compared in our SCF results.

The origin-dependent dipole moment (Table III) has been computed with reference to the center of the CC distance. In the bridged series the positive end of the dipole is directed toward the proton.

Localization and Population Analysis

Bridge Structure. Both the optimum bridge structure, which we discuss first, and the *R* variation of the bridged structure localize to resemble an intermediate between ethylene[13a] and diborane.[13a] These bridge structures localize uniquely to four CH bonds, and either to a CC bond and a CHC bridge bond or to two CC

---

[16] W. E. Palke and W. N. Lipscomb, *J. Chem. Phys.*, 45, 3948 (1966).

[17] J. H. Hall, Jr., D. S. Marynick, and W. N. Lipscomb, *Inorg. Chem.*, 11, 3126 (1972).

[18] These studies, and wave functions of the present paper, are to be summarized in D. A. Dixon, Ph.D. Thesis, Harvard University, to be submitted. A configuration interaction calculation with the minimum basis set including all single and double excitations from valence shells gives a ΔE of 3.9 kcal/mol favoring the open structure. Thus, the bridge structure has gained 8 kcal/mol of energy through configuration interaction.

Table II. Energetics (au)[a]

	Kinetic energy	Nuclear attraction	Nuclear repulsion	Two electron	Total SCF	$-E/T$	Interorbital coulomb[b]	Exchange[c]	Self-repulsion
2.17 (opt, bridge)	77.567	−251.540	38.054	57.762	−78.157	1.0076	62.949	−5.186	6.528
3	77.596	−251.585	38.025	57.854	−78.110	1.0066	62.985	−5.131	6.558
4	77.647	−250.153	37.052	57.432	−78.022	1.0048	62.554	−5.122	6.521
6	77.803	−249.042	35.940	57.381	−77.918	1.0015	62.528	−5.148	6.489
8	77.844	−248.492	35.334	57.422	−77.892	1.0006	62.584	−5.162	6.483
10	77.849	−248.089	34.957	57.397	−77.886	1.0005	62.564	−5.167	6.480
12	77.848	−247.800	34.701	57.367	−77.884	1.0005	62.537	−5.170	6.477
13	77.848	−247.687	34.602	57.355	−77.883	1.0005	62.526	−5.170	6.476
$C_2H_4(\infty)$	77.879	−248.022	33.382	58.904	−77.856	0.9997	64.131	−5.228	6.570
(opt open)	77.587	−249.509	36.882	56.864	−78.176	1.0076	58.812	−1.948	9.797

[a] 1 au of energy is 27.21 eV or 627.5 kcal/mol. [b] $\Sigma_{i>j}4(ii|jj)$. [c] $\Sigma_{i>j}2(ij|ij)$. [d] $\Sigma_i(ii|ii)$.

Table III. Dipole Moments

R, au	Dipole	Dipole direction
2.17	1.17	z
3	1.80	z
4	3.40	z
6	7.98	z
8	12.32	z
10	16.15	z
12	19.82	z
13	21.64	z
C_2H_4	0.0	
Bridge	1.97	x (0.0) y (1.94 D) z (0.34 D)

[a] The origin has been chosen at the center of the C–C bond, inasmuch as the dipole moment of an ion is origin dependent.

Table IV. Localization Energetics

R	Coulomb	Exchange	Self-repulsion	2nd deriv test
2.17	58.264	−0.502	11.213	−0.497
3	58.369	−0.515	11.174	−0.384
4	57.961	−0.529	11.114	−0.246
6	57.938	−0.557	11.080	−0.055
8	57.983	−0.562	11.084	−0.039
10	57.958	−0.561	11.086	−0.053
12	57.927	−0.560	11.086	−0.060
13	57.915	−0.560	11.086	−0.063
C_2H_4	59.458	−0.554	11.243	−0.247

Table V. Net Mulliken Charges (e) on H and C atoms

R, au	Charge H^+	Charge H	Charge C
2.17	0.21	0.22	−0.05
3	0.23	0.21	−0.04
4	0.32	0.19	−0.05
6	0.52	0.16	−0.08
8	0.61	0.14	−0.09
10	0.64	0.14	−0.09
12	0.65	0.13	−0.09
13	0.66	0.13	−0.09
C_2H_4		0.08	−0.16
Open	0.21	0.24 (1) 0.19 (3)	0.21 (1) −0.27 (2)

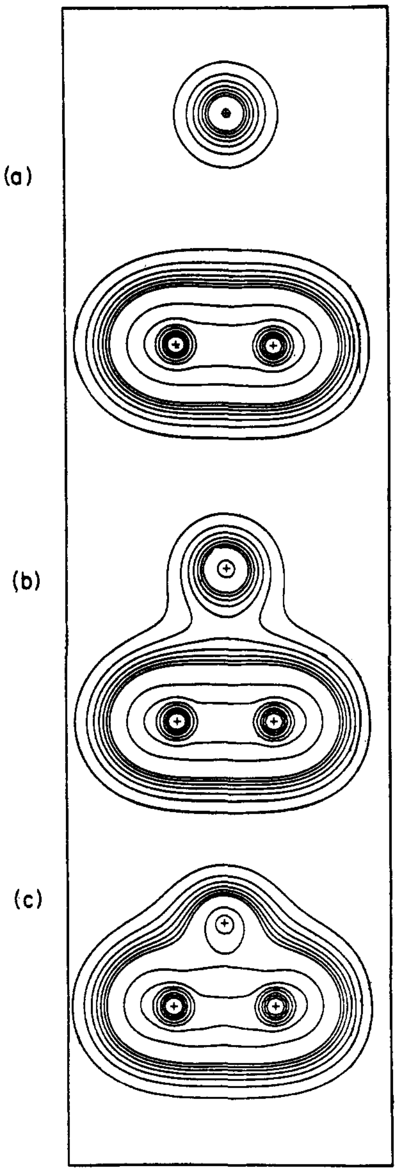

Figure 1. Total electron density maps in the CH^+C plane. Bridge series. The crosses represent the atomic centers. (a) Proton at 6 au from center of planar C_2H_4; (b) proton at 4 au from center of planar C_2H_4; (c) optimized bridged structure (C_2H_4 no longer planar). The contour levels in e/au^3 are 10.0, 5.0, 2.5, 1.0, 0.5, 0.25, 0.15, 0.07, 0.06, 0.05, 0.04, 0.03, 0.02, and 0.01. The total Mulliken population on the proton at 6 au in a is only 0.44 e.

bent (τ) bonds like those in ethylene. The localization energy quantities are given in Table IV. The total density (Figure 1), the CC bond (Figure 2), and the CHC bridge bond (Figure 3) show an interesting variation with distance of the proton.

In the optimum bridged structure, the bridge hydrogen is somewhat positive and the carbons are slightly negative (Table V). However, the CHC three-center bond (Figure 3c) has a higher electron density around the proton than around the carbons, as seen by the

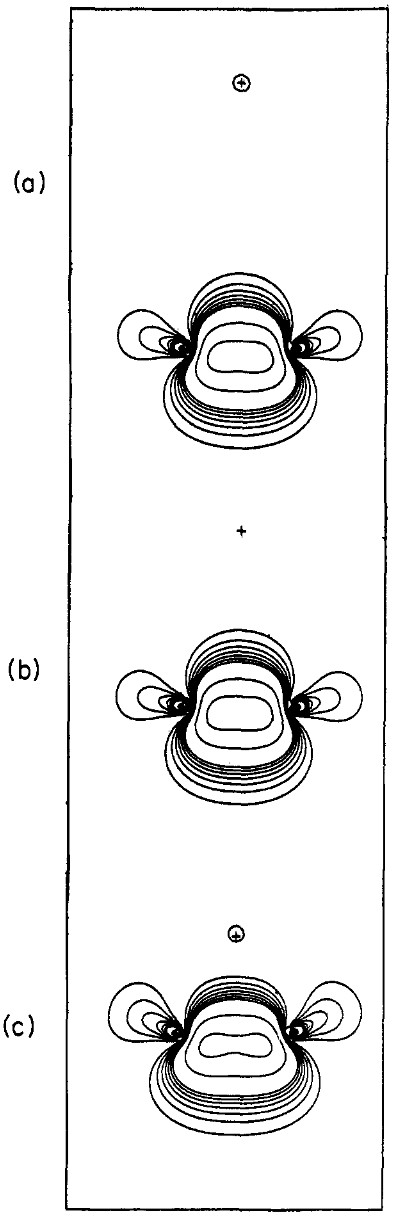

Figure 2. Electron density maps. C–C localized bond-bridge series. For a, b, and c geometries and contour levels, see legend to Figure 1.

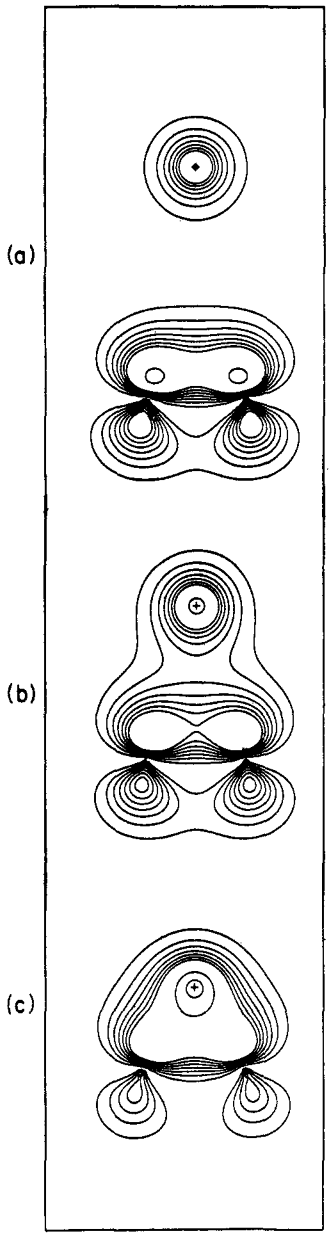

Figure 3. Electron density maps. CHC localized bond-bridge series. For a, b, and c geometries and contour levels, see legend to Figure 1.

localized orbital populations of 0.60 electron (e) for C and 0.82 e for H. For comparison, diborane has populations of 0.51 e for B and 1.02 e for H,[13a] in reasonable expectation from the smaller nuclear charge of B as compared with C. The nonbridge H atoms of the optimized bridge structure of $C_2H_5^+$ show localized populations of 1.22 e on C and 0.79 e on H, as compared with the values of 1.08 on C and 0.94 on H in C_2H_4. Thus the hydrogens are more positive in $C_2H_5^+$ than in C_2H_4, as might be expected, and it is interesting that the C atoms have appreciably more electrons from the C–H bonds in $C_2H_5^+$ than they do in C_2H_4. We note especially that about 80% of the positive charge in $C_2H_5^+$ is distributed among the four terminal H atoms in a Mulliken charge analysis. However, we caution that this analysis tends to place excess electrons on atoms in higher coordination situations, and therefore prefer total densities when comparing bridge and terminal hydrogen atoms.

The remainder of this section is concerned with the effect of approach of the proton on the ethylene molecule to form $C_2H_5^+$ (Tables V and VI, and Figures 4

Table VI. Population Analysis of Localized Orbitals for Bridged $C_2H_5^+$ and C_2H_4

	Essentially C–C[a]			C–H_b–C		
	C	H_b	C	C	H_b	C
2.17	1.02	0.02	1.02	0.60	0.82	0.60
3	1.01	0.00	1.01	0.61	0.78	0.61
4	1.01	0.01	1.01	0.67	0.67	0.67
6	1.00	0.03	1.00	0.78	0.44	0.78
8	0.94	0.15	0.94	0.88	0.25	0.88
10	0.93	0.16	0.93	0.91	0.20	0.91
12	0.93	0.16	0.93	0.92	0.19	0.92
13	0.93	0.16	0.93	0.92	0.18	0.92
C_2H_4	1.01		1.01	1.01		1.01

[a] There is an antibonding interaction between this C–C bond and the bridge hydrogen, H_b.

Table VII. Analysis of Localized Orbitals of C–C, C–H–C, and C–H Bonds into 2s, $2p_x$, $2p_y$, and $2p_z$ Components on C Atoms for Bridged $C_2H_5^+$ and C_2H_4

	C–C[a]			CHC[a]			CH[b]		
	2s	$2p_z$	$2p_y$	2s	$2p_z$	$2p_y$	2s	$2p_x$	$2p_y$
2.17	0.31	0.15	0.56	0.06	0.48	0.06	0.44	0.59	0.20
3	0.33	0.07	0.62	0.04	0.54	0.04	0.43	0.58	0.20
4	0.34	0.04	0.63	0.03	0.62	0.02	0.43	0.58	0.20
6	0.34	0.06	0.60	0.04	0.70	0.05	0.41	0.56	0.19
8	0.24	0.30	0.40	0.16	0.50	0.23	0.40	0.55	0.20
10	0.22	0.37	0.35	0.18	0.45	0.28	0.39	0.55	0.20
12	0.21	0.39	0.33	0.19	0.44	0.29	0.39	0.55	0.20
13	0.21	0.40	0.33	0.19	0.43	0.30	0.39	0.55	0.20
C_2H_4	0.21	0.50	0.31	0.21	0.50	0.31	0.37	0.52	0.20

[a] There is no $2p_x$ component. [b] There is no $2p_z$ component.

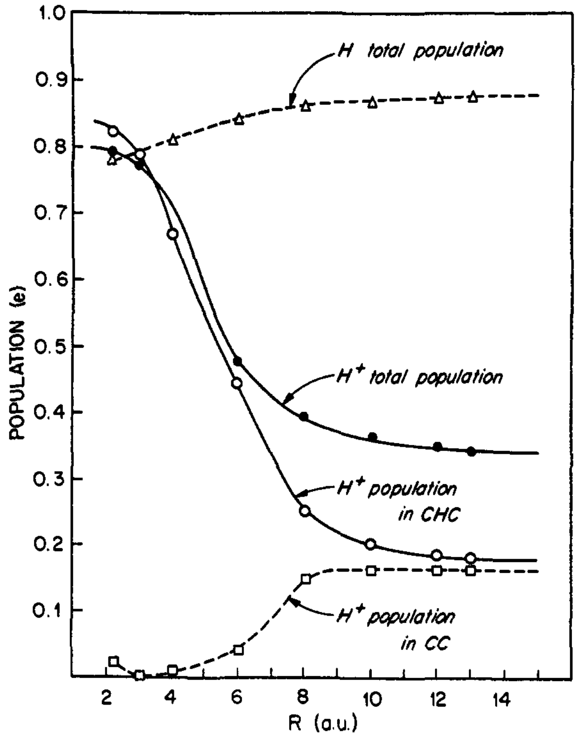

Figure 4. Populations and charge on H's plotted against R, the distance of approach of H^+ to the center of the C–C line: (○) H^+ population in CHC; (□) H^+ population in CC; (●) H^+ total population; (△) H total population.

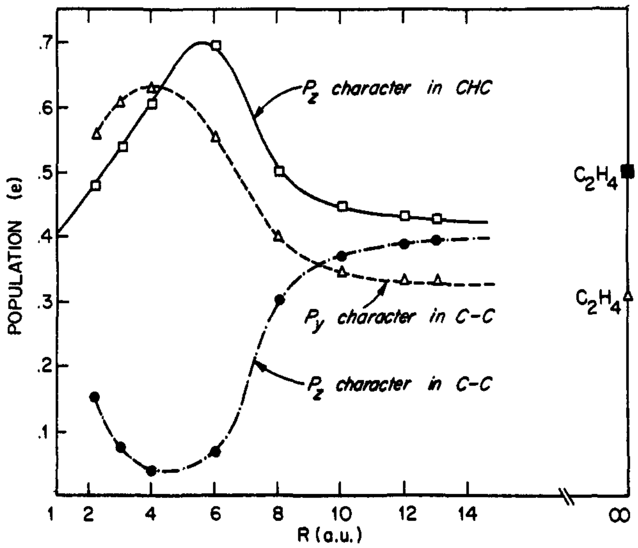

Figure 5. Atomic orbital components of CC and CHC localized bonds as a function of R: (△) p_y character in CC; (●) p_z character in CC; (□) p_z character in CHC.

and 5). The two localized π bonds of ethylene ($R = \infty$) have no proton populations and have large p_z components (Table VII). At $R = 13$ au the proton is almost equidistant from the two π bonds of C_2H_4, and perturbs them about equally, yielding the small proton populations of 0.16 e in the CC bond and 0.18 e in the CHC bond (Table VI and Figure 4). We now analyze in the next paragraphs the effect that the approach of the proton has on the localized CC bonds of C_2H_4 that become the CC bond and the CHC bond of $C_2H_5^+$.

As the proton approaches, the CC bond loses p_z character and gains p_y and 2s character (Figure 5) as it becomes more nearly sp. The effect at 6 au is well shown in Figure 2a. Further approach of the proton changes this bond from nearly linear sp again to a bent bond, which shows noticeable p_y lobes (Figure 2). At the optimized bridge geometry, the CC bond is thus again bent, showing a decrease in 2s and p_y character and an increase in p_z character (Figures 2c and 5). The loss of electron density on the side of the proton is noted in this CC bond (*cf.* Figure 2c with Figures 2a and 2b) as the proton approaches, and a tendency can be seen for spreading of the electron density toward the CH bonds.

The CHC bond undergoes an even more striking transformation. At large R, the C atoms of this bridge bond have slightly more p_z character and less p_y character than are present in the CC bond (Table VII). As the proton–origin distance decreases, the amounts of p_y and 2s character decrease. Between $R = 8$ au and $R = 6$ au a large change occurs as the carbon components of the bond become predominantly p_z orbitals (Figures 3a and 5). The amount of p_y and 2s character reaches a minimum at $R = 4$ au (Figure 3b). At the optimum geometry there is a slight increase in p_y and 2s character (Figure 3c and Table VII). The p_z component reaches a maximum near $R = 6$ au (Figure 5) and then decreases as the electrons redistribute themselves over the whole CHC bond until the hydrogen has more electron population (0.82) than do the carbons (0.60). This effect supports our calculation of the turning point distance R_{TP} which is discussed below.[19] Note the distinct maxima for the two p_z orbitals on the

(19) As noted by us, and by a Referee, these results suggest that the electron density responds to the incoming proton at about 3.7 Å, while the energy–distance plot indicates that the C–C bond changes noticeably when the incoming proton reaches about 1.6 Å. If this result is general, simplified perturbation schemes may be useful in treating reactivities of certain classes of molecular species.

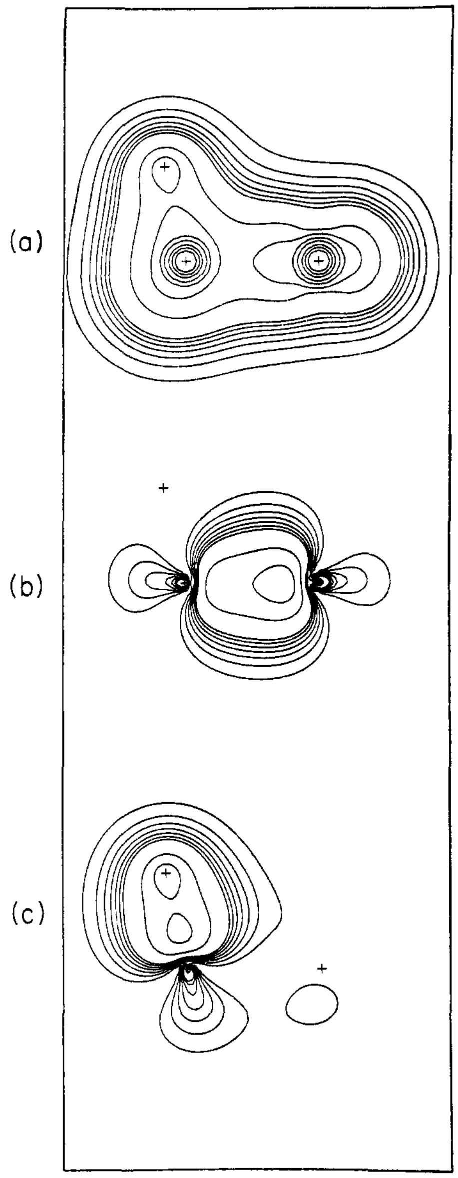

Figure 6. Electron density maps for open $C_2H_5^+$ in the CH^+C plane. The crosses represent the atomic centers. (a) Total density; (b) localized C–C bond; and (c) localized C–H bond. Note that the very slight hyperconjugation toward the π orbital of the CH_2 group is on the side (bottom) opposite the newly formed C–H bond. Contour levels are the same as in Figure 1.

proton side at $R = 6$ au (Figure 3a). These maxima are more connected due to an increase in mixing as the proton reaches 4 au; this shows a strong valence interaction (Figure 3b). Finally, at the equilibrium distance the three-center CHC bond is completely formed (Figure 3), showing a maximum of electron density at the proton, but distorted toward the origin at the midpoint of the CC line. On the side opposite the proton, this localized CHC bond shows a marked decrease in electron density and distinct p_z lobes at the equilibrium distance (Figure 3c), indicating that the $p_z \cdots p_z$ interaction of the original CC bond is largely replaced by the three-center interaction as the proton approaches from about 4 to 2.17 au. The slight increase of density along the CC axis reflects the slight increase in p_y and 2s character in the final stages of bond formation as the proton approaches (Figure 3c).

These changes in the CC and CHC bonds of the bridged structure can be interpreted as follows. As the proton moves toward ethylene, the τ bond on the side of the proton is attracted by a Coulomb force, resulting in an increase of p_z character. Overlap between C and C within the upper τ bond is decreased, and the lower τ bond thus acquires more bonding along the C–C direction. As the proton begins to form the CHC bridge bond, the p_z character of the corresponding τ bond reaches a maximum, and its electrons begin to occupy the vacant orbital of the proton. However, as the proton comes close to its optimum position the CHC bond moves closer toward the CC line, and hence becomes more like the original τ bond of ethylene. Now the p_z orbitals are bent slightly inward toward the proton, the bond overlap between CHC and CC bonds increases, and thus the CC bond becomes more bent having an increase in p_z character and a decrease in p_y and 2s character.

Open Structure. The results of this localization are reasonably like those for saturated hydrocarbons, except, of course, for the vacant orbital (Table VIII and Figure 6). The CH bonds of the CH_2 group (C_1 in Chart I) are very like those in the optimized bridge structure. The two symmetry-related H atoms of the CH_3 group are essentially formed from a 2s–p_x hybrid on atom C_2, and the CH^+ bond to the unique hydrogen is bonded to C_2 mostly through p_z, but some 2s character (0.3 e, Table VIII) is also present (Figure 6c). This CH^+ bond is very different from that in the bridged structure where no 2s character is present, and the localized bond density shows an interesting double maximum along the C–H^+ line (Figure 6c). Although this CH^+ bond is not symmetric about the C–H^+ line, but skewed toward C_1, the very small p_z contribution of 0.1 e from C_1 indicates very little p_z–p_z bonding. Thus there is very little donation from the localized CH^+ bond into the vacant orbital of C_1 as shown clearly in Figure 3c. It is interesting that the small amount of hyperconjugation which does occur is on the side of the CC line opposite that of the proton. Total populations bear this out, showing 0.14 e in p_z of C_1 and 1.10 e in p_z of C_2. By contrast, the p_z orbital of each C of the bridge structure has a population of 0.64 e.

Table VIII. Results for Localized Bonds in Open $C_2H_5^+$

Coulomb energy, au	Exchange energy, au	Self-repulsion energy, au	2nd derivative	
57.340	−0.476	11.270	−0.715	
		Populations (e)		
		Atom 1	Atom 2	
C_1–H		1.24	0.78	
C_2–H		1.17	0.84	
C_2–H^+		1.11	0.82	
C_1–C_2		1.21	0.83	
		AO populations (e)		
Bond	2s	$2p_z$	$2p_x$	$2p_y$
C_1H	0.45		0.59	0.21
C_2H	0.35	0.15	0.58	0.10
C_2H^+	0.29	0.79		0.03 (0.10 C_1 $2p_z$)
C_1C_2	0.47 C_1 0.20 C_2			0.75 C_1 0.63 C_2

The CC bond of the open structure is predominantly 2s and p_y in character, coaxial with the CC line, and

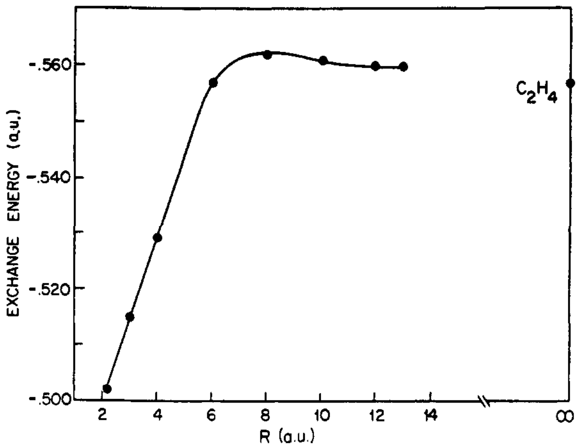

Figure 7. Exchange energy for the localized structures as a function of R.

polar having greater electron density on C_1 (Figure 6b). Hybridizations are $sp^{1.6}$ on C_1 and $sp^{3.1}$ on C_2. For comparison, we note that hybridizations are $sp^{9.8}$ in the bridge bond of $C_2H_5^+$, $sp^{2.3}$ in the CC bond of $C_2H_5^+$, and $sp^{3.9}$ in C_2H_4. Mulliken charge analysis shows C_1 at +0.21 e and C_2 at −0.27 e, opposite in polarity to that of the CC bond, and substantiating the very small donation into the p_z orbital of C_1.

The ambiguity of proton approach to form the open structure was not investigated, but we suggest that as the proton approaches C_2, electrons in the bonding π orbital of ethylene will flow from p_z of C_1 into p_z of C_2 until the final distribution is reached at the equilibrium distance.

Turning Point Distance. As the proton approaches an ethylene molecule the early stages suggest that the ethylene wave function is polarized by the field of the proton. However, a strong valence interaction begins at a distance which we define as the turning point. This distance is of importance in ion–molecule collision theories which yield cross sections, and which often are expressed in terms of an impact parameter, b_0. For example, b_0 is often calculated from the Langevin expression (assuming an R^{-4} potential)

$$b_0 = (2\alpha e^2/E)^{1/4} \tag{1}$$

where α is the average polarizability of the neutral molecule and E is the relative kinetic energy of approach at large distances.[20] For collision at thermal energies ($E = {}^3/_2kT$) of a proton and ethylene ($\alpha = 42.6 \times 10^{-25}$ cm^3),[21] eq 1 yields $b_0 = 7.5$ Å. The radius of the reaction sphere is $b_0/\sqrt{2} = 5.3$ Å.

The onset of significant valence interaction occurs at somewhat shorter distances. A summary of the behavior of various valence criteria *vs.* R (Figures 7 and 8, and Table IV) yields the following turning points (R_{TP}). An approximate turning point is thus 7 au = 3.7 Å. Below this distance the $C_2H_5^+$ ion is bound by covalent interactions, while above this distance the proton merely perturbs the ethylene molecule.

Property	R_{TP}, au
Exchange energy (Figure 7)	8−
Second derivative test (Figure 8)	8−
Proton population, CC bond (Figure 4)	7
Self-repulsion energy	7−

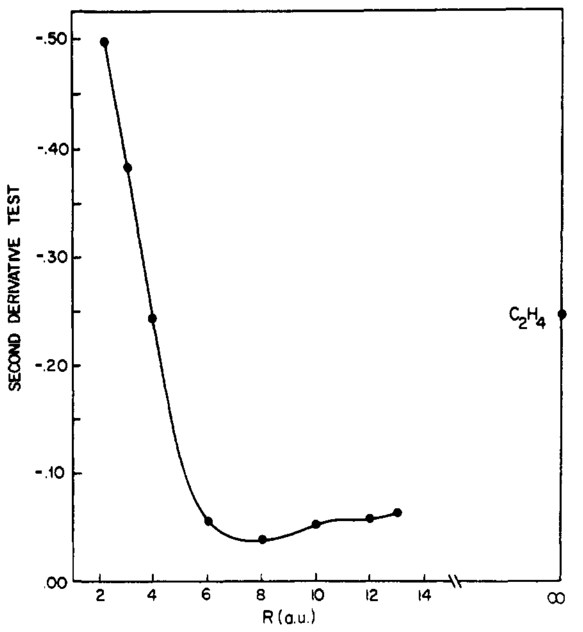

Figure 8. Second derivative test[13b] as a function of R.

Virtual Molecular Orbitals and Reactivity

Bridge Structure. Energies of the lowest unoccupied molecular orbitals are shown as a function of R in Table IX. The totally symmetric antibonding orbital (type 1) is primarily the proton 1s orbital in an antibonding interaction with a relatively small fraction of the pair of p_z orbitals on the C atoms. As the proton approaches ethylene, this orbital increases in energy from −0.389 au at 13 au to 0.113 au at 2.17 au. The strong antibonding interaction of this vacant orbital arises from the bonding interaction of the filled orbital discussed in previous parts of this paper. Of course, at large R, the population of electrons on this proton is quite small, and the energy resembles that of a vacant 1s orbital on hydrogen.

Table IX. Eigenvalues (au) of Lowest Virtual Molecular Orbitals

R	Type 1[a]	Type 4[b]
2.17	0.113	−0.097
3	−0.142	−0.060
4	−0.262	−0.028
6	−0.357	0.032
8	−0.381	0.071
10	−0.387	0.092
12	−0.389	0.106
13	−0.389	0.112
C_2H_4		0.281
Open	−0.202	

[a] Totally symmetric. [b] Antisymmetric in the xz plane, and antisymmetric about the twofold axis C_z (see Figure 1).

The lowest unoccupied orbital of symmetry type 4 (antisymmetric both about the C_2 axis and in the xz plane) is mostly an antibonding interaction of p_z of C_1 with p_z of C_2. As the proton approaches, the energy goes from 0.10 au at 13 au to −0.10 au at 2.17 au, and, hence, this orbital is the reasonable candidate to accept

---

(20) D. P. Stevenson in "Mass Spectrometry," C. A. McDowell, Ed., McGraw-Hill, New York, N. Y., 1963, p 589.

(21) J. O. Hirschfelder, C. F. Curtiss, and R. B. Byrd, "Molecular Theory of Gases and Liquids," Wiley, New York, N. Y., 1954, p 950.

the electron pair of R^- if the second step of the Markovnikov addition adds R^- to bridged $C_2H_5^+$.

Open Structure. The lowest unoccupied orbital is symmetric in the plane of open $C_2H_5^+$ (type 1), has a negative eigenvalue (Table IX), and is almost entirely p_z of C_1 (its normalized coefficient is 0.98). This nearly vacant orbital would be an ideal receptor for a lone pair upon addition of R^- to open $C_2H_5^+$ in the Markovnikov addition. Although both the bridge and open structures of $C_2H_5^+$ have favorable orbitals and eigenvalues for addition of R^-, the open structure seems more favorable from these results. Hence, if the bridge structure of $C_2H_5^+$ is more stable than the open form, we suggest that a transformation from the bridge to the open form may occur during the addition of R^-. However, a detailed study is required. Hence, we are presently examining theoretically the addition of H^- to $C_2H_5^+$.

Transferability. The use of localization procedures for obtaining transferable bonds[22] leads us to compare our localized bonds with one another and with those on hydrocarbons. It is most appropriate to compare the C_1H bonds of the CH_2 group in open $C_2H_5^+$ with the CH bonds of the bridge structure (Tables VII and VIII). Even though C_1 (open) is positive (0.21 e), while C (bridge) is negative (−0.05 e), the CH bonds are remarkably alike, having the same hybridization ($sp^{1.8}$) and differing only slightly in 1s (of H) and p_y (of C) character. A survey of all of our results shows variations of electron populations of 0.01 e in p_y and of 0.08 e in p_x and 2s of C. Populations of 1s of H vary by 0.16 e in the opposite direction from that of the changes in p_x and 2s of C. The CH bonds in ethylene are $sp^{2.0}$ hybrids and have atomic orbital coefficients close to those in the bridge and open structures even though the charge distribution is quite different. These results suggest that CH bonds, in approximately the same geometry with respect to a CC bond, may be transferable. However, CC bonds which are more reactive are not transferable.

Acknowledgment. We wish to thank the Office of Naval Research for support of this research, and we are grateful to D. S. Marynick and J. H. Hall, Jr., for helpful advice. We also thank R. M. Stevens for the use of his SCF program.

---

[22] (a) C. Trindle and O. Sinanoglu, *J. Chem. Phys.*, **49**, 65 (1968); (b) C. Trindle and O. Sinanoglu, *J. Amer. Chem. Soc.*, **91**, 853 (1969).

Electronic Structure of Thieno[3,4-*d*]thiepin

R. Gleiter,*[1] E. Schmidt,[1] P. Johnson,[2] and D. O. Cowan[2]

Contribution from Physikalisch-Chemisches Institut der Universität Basel, Basel, Switzerland, and the Chemistry Department, The Johns Hopkins University, Baltimore, Maryland 21218. *Received May 15, 1972*

Abstract: CNDO/2 and extended Hückel calculations of thieno[3,4-*d*]thiepin (**1**) reveal a small difference in energy between a planar and a nonplanar structure, both with bond alternation. The electronic spectrum of **1** was measured with polarized light using the stretched-film technique. The first four bands are assigned to $\pi^* \leftarrow \pi$ transitions on the basis of PPP–CI calculations. These bands are correlated with the first four bands of azulene. For the first transition a hypsochromic shift is predicted upon methyl substitution in all positions.

Schlessinger[3a–c] has recently reported the synthesis of the novel $4n$-π-electron heterocycle, thieno[3,4-*d*]thiepin (**1**). The relative stability of **1** was attributed to an extensive delocalization in the π system, and it has been proposed that this delocalization may be due to charge-separated resonance structures summed up by **2**. In order to ascertain the nature of the π-electron delocalization in **1**, an X-ray structure analysis has been carried out.[3b] A disordered structure similar to that of azulene was found, and this hampered a complete analysis. It was reported that the molecule is almost planar in the crystal and that the length of the transannular bond is 1.46 Å.

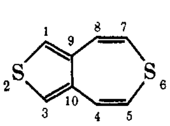

1

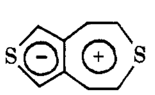

2

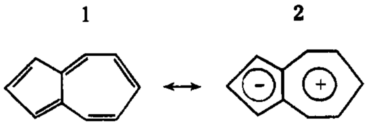

4a **4b**

In an attempt to learn more about the electronic structure of this 12π-electron heterocycle,[4] the electronic spectra of **1** in cyclohexane and ethanol, the polarization spectra (uv) in stretched polymer sheets, and the fluorescence spectrum in cyclohexane were measured.

In addition, CNDO/2,[5] EH,[6] and PPP[7] calculations

---

[1] Physikalisch-Chemisches Institut der Universität Basel.

[2] The Johns Hopkins University.

[3] (a) R. H. Schlessinger and G. S. Ponticello, *J. Amer. Chem. Soc.*, **89**, 7138 (1967); (b) T. D. Sakore, R. H. Schlessinger, and M. H. Sobell, *ibid.*, **91**, 3995 (1969); (c) R. H. Schlessinger and G. S. Ponticello, *Tetrahedron Lett.*, **25**, 3017 (1968).

[4] For a recent review on $4n$-π-electron heterocycles, see L. A. Paquette in "Nonbenzenoid Aromatics," Vol. I, J. P. Snyder, Ed., Academic Press, New York and London, 1969, p 249.

[5] J. A. Pople and D. L. Beveridge, "Approximate Molecular Orbital Theory," McGraw-Hill, New York, N. Y., 1970, and references therein.

[6] R. Hoffmann, *J. Chem. Phys.*, **39**, 1397 (1963); R. Hoffmann and W. N. Lipscomb, *ibid.*, **36**, 2179, 3489 (1962); **37**, 2872 (1962). The Slater exponent for hydrogen used was 1.3.

[7] R. G. Parr, "Quantum Theory of Molecular Electronic Structure," W. A. Benjamin, New York, N. Y., 1964, and references therein.